Available online at www.sciencedirect.com
SCIENCE DIRECT®
Biochemical and Biophysical Research Communications 329 (2005) 296–304
BBRC
www.elsevier.com/locate/ybbrc

Increase of smooth muscle cell migration and of intimal hyperplasia in mice lacking the α/β hydrolase domain containing 2 gene

Keishi Miyata [a,b], Yuichi Oike [c], Takayuki Hoshii [a], Hiromitsu Maekawa [c], Hisao Ogawa [b], Toshio Suda [c], Kimi Araki [a], Ken-ichi Yamamura [a,*]

[a] *Department of Developmental Genetics, Institute of Molecular Embryology and Genetics, Kumamoto University School of Medicine, 4-24-1 Kuhonji, Kumamoto 862-0976, Japan*
[b] *Department of Cardiovascular Medicine, Graduate School of Medical Sciences, Kumamoto University, 1-1-1 Honjo, Kumamoto 860-8556, Japan*
[c] *Department of Cell Differentiation, The Sakaguchi Laboratory, Keio University School of Medicine, Tokyo 160-8582, Japan*

Received 19 January 2005

Abstract

Multiple steps, including the migration of vascular smooth muscle cells (SMCs), are involved in the pathogenesis of atherosclerosis. To discover genes which are involved in these steps, we screened mutant mouse lines established by the exchangeable gene trap method utilizing X-gal staining during their embryonic development. One of these lines showed strong reporter gene expression in the vitelline vessels of yolk sacs at embryonic day (E) 12.5. The trap vector was inserted into the fifth intron of α/β hydrolase domain containing 2 (*Abhd2*) gene which was shown to be expressed in vascular and non-vascular SMCs of adult mice. Although homozygous mutant mice were apparently normal, enhanced SMC migration in the explants SMCs culture and marked intimal hyperplasia after cuff placement were observed in homozygous mice in comparison with wild-type mice. Our results show that *Abhd2* is involved in SMC migration and neointimal thickening on vascular SMCs.

Keywords: Gene trap; α/β hydrolase protein; Abhd2; Smooth muscle cell; Migration; Cuff placement model; Neointimal hyperplasia; Atherosclerosis; Alveolar type II cell; Hepatocyte

Smooth muscle-associated protein 8 (smap8), epoxide hydrolase and retinoid-inducible serine carboxypeptidase (RISC), which are members of the α/β hydrolase family, are all reported to be related to vascular smooth muscle cell proliferation and the progression of atherosclerosis [1–3]. In addition, one of these members, epoxide hydrolase, has been found to play an important role in the pathogenesis of atherosclerosis as revealed by a human polymorphism study [4].

The α/β hydrolase fold family consists of hydrolytic enzymes of widely differing phylogenetic origin. Each of these family members has the same protein fold, termed as the α/β hydrolase fold [5,6]. The core of each enzyme is similar: an α/β-sheet of five to eight β-sheets connected by α-helices to form an α/β/α sandwich. In most of the family members, the β-strands are parallel; some though show an inversion in the order of the first strands, resulting in an antiparallel orientation. These enzymes diverge from a common ancestor so they preserve the arrangement of the catalytic residues, not the binding sites. They all have a nucleophile–histidine–acid catalytic triad, the elements of which are borne on loops which are the best-conserved structural features in the fold. Only the histidine in the catalytic triad is completely conserved, with the nucleophile and acid loops containing more than one type of amino acid. The nucleophile can be a Ser, Cys or Asp residue while the acid loops accommodate an Asp or Glu residue.

* Corresponding author.
E-mail address: yamamura@gpo.kumamoto-u.ac.jp (K. Yamamura).

0006-291X/$ - see front matter © 2005 Elsevier Inc. All rights reserved.
doi:10.1016/j.bbrc.2005.01.127

In mice, three cDNA encoding proteins containing an α/β hydrolase fold were cloned from lung cDNA [7]; they were named as lung α/β hydrolase (Labh) 1, 2, and 3. These are now termed as abhydrolase domain containing (Abhd) 1, 2 or 3. RT-PCR analyses showed that these three genes are widely, but differentially expressed in many tissues. The expression of *Abhd1* and *Abhd3* was highest in the liver and lowest in the spleen, whereas the expression of *Abhd2* was high in the testis and the spleen. The *Abhd1* catalytic triad was identified as Ser211, Asp337, and His366. In addition, all three Abhd proteins are shown to have a single predicted amino-terminus transmembrane domain. Although proteins in this family generally act as enzymes such as dienelactone hydrolases, haloalkane dehalogenases, carboxypeptidases, acetylcholinesterases, or lipases, the specific functions of the three Abhd proteins are unknown.

The gene trap strategy using embryonic stem (ES) cells is a powerful method for both the identification of genes and the subsequent establishment of mutant lines [8,9]. We performed gene trap insertional mutagenesis using the trap vector pU-Hachi, and isolated a clone, Ayu8025, in which the trap vector was inserted into the *Abhd2* gene. In the present study, we found that *Abhd2* deficient mice appear normal without any apparent defect in their vascular development; however, they showed both enhanced SMC migration in the explants SMCs culture and marked intimal hyperplasia after cuff placement, suggesting that *Abhd2* in vascular SMCs negatively regulates the formation of neointimal hyperplasia due to vascular injury.

Materials and methods

Generation of gene trap mice. The Ayu8025 gene trap line was isolated as previously described [10]. Chimeric mice were produced by aggregating ES cells with eight-cell embryos. The chimeric male mice were backcrossed to C57BL/6 females to obtain F1 heterozygotes. In this study, we used mice of the F9 generations.

Cloning of genomic DNA and genotyping. Plasmid rescue was performed to obtain flanking genomic DNA as described [10]. DNA samples for genotyping were isolated from the tails of embryos, newborn mice, and adult mice for genotyping. Genotyping was done with PCR using tail genomic DNA as a template. For wild-type alleles, a 5′ primer, G1 (5′-GAGGTCCTCTGCTCCCTGTAT-3′), located in the deleted region by the trapping event, and a 3′ primer, G2 (5′-GTAAGAGCTCCCTTGACTTTCC-3′), located in the sixth exon, were used to generate a 663 bp wild-type fragment. To detect the trap allele, another 5′ primer, G3 (5′-AGCGGATAACAATTTCACAC AGGA-3′), located in the pUC19, and the 3′ primer G2 were used to generate a 425 bp fragment. For PCR analysis, the DNA was subjected to 30 cycles (30 s at 94 °C; 60 s at 59 °C; and, 60 s at 72 °C) using 0.5 U of *Taq* polymerase (Perkin–Elmer, Foster City, CA).

RNA analysis. Rapid amplification of cDNA ends (RACE) using the 5′ and 3′ RACE system (Invitrogen, Carlsbad, CA) was utilized to characterize the trapped gene, 5′ or 3′, as described previously [11]. Total RNAs were extracted from various tissues and were used for RT-PCR analysis. For Northern blot analysis, 10 μg poly(A)$^+$ RNAs isolated from various tissues were purified with the OligotexTM-dT30 mRNA purification kit (Takara Shuzo, Kyoto, Japan), as described previously [12]. An *Abhd2* cDNA probe (nucleotides 52–550) was prepared using DIG-labeled antisense probe riboprobes (Roche, Germany) and used for the Northern blot analysis. Primers used in the RT-PCR include the following: A1 (5′-GTTGGACTGCTGGAGTC AAT-3′) located in the 1st exon (nucleotide number 48–67); A2 (5′-AC TGCTTCTCGCTGTGGTTG-3′) located in the fifth exon (nucleotide number 586–605); B2 (5′-TCCTCTTTGTTAGGGTTCTTC-3′) located in the splice acceptor of the trap vector; C1 (5′-GACATATCCC CAGACCCAGC-3′) located in the sixth exon (nucleotide number 763–782); C2 (5′- ACAGCCGGCTCAAG-3′) located in the eighth exon (nucleotide number 1051–1064); D1 (5′-CGACCCCTTGGTGC ACGAAAG-3′) located in the 10th exon (nucleotide number 1213–1233); and D2 (5′-CCAGGGAGAGCCGCCTACTTG-3′) located in the 11th exon (nucleotide number 1594–1604). Changes in the mRNA levels of *Abhd2* in the cuff-injured areas were measured by reverse transcriptase-polymerase chain reaction (RT-PCR). The total RNA was extracted from normal and cuff-injured femoral arteries and RT-PCR was performed using two set primers to generate a 432 bp fragment: 5′-TCGACCTCTTCGAGCCCCTG-3′ located in the fourth exon (nucleotide number 513–532); and 5′-CCTGCGGCACTGGTC-3′ located in the seventh exon (nucleotide number 929–944). Each RNA quantity was normalized to its respective glyceraldehyde-3-phosphate dehydrogenase (GAPDH) mRNA quantity.

In situ hybridization. In situ hybridization analyses were performed on whole mounts and sections of staged embryos as described previously [13] and on adult tissue section samples utilized a VENTANA in situ hybridization machine. DIG-UTP-labeled antisense and control sense probe riboprobes (Roche, Germany) were synthesized by transcription from the pGEM-T vector plasmid with SP6 or T7 on RNA polymerase and then purified on Quick Spin Columns (Bio-Rad, Hercules, CA).

Histochemistry, immunohistochemistry, and β-galactosidase staining. For immunofluorescent detection, tissues were fixed with 4% paraformaldehyde and then washed with three rinses of PBS. Sections were incubated in 4% normal goat serum at room temperature for 1 h followed by 12–15 h in a primary antibody solution of PBS/Triton. The α-SMA immunoreactivity was detected by an α-SMA/HRP monoclonal antibody (Dako, Carpinteria, CA) diluted 1:500, followed by anti-rat biotin-labeled second antibodies at a 1:500 dilution. The β-galactosidase staining for sample was performed as described [14].

Preparation of explants, proliferation, and migration assay. Mice aorta explant cultures were performed as described [15]. Thoracic aortas of adult mice (age 10–12 weeks, wild-type, and homozygote mice) were dissected and the endothelium and periadvential fat was removed by gentle abrasion. Then, the aortas were cut into 2 × 2 mm explants. The explants were individually plated with the lumen side down into collagen type I-coated 12-well multiplates and cultured in 150 μL Dulbecco's modified Eagle's medium (DMEM) containing 10% fetal bovine serum, penicillin/streptomycin, and 2-mercaptoethanol. To characterize the cells migrating from explants, cells were fixed and stained for SM α-actin. For the experiments, SMCs in a subconfluent state at the third and fifth passage were used.

For the proliferation assay, SMCs were plated on collagen type I-coated 96-well plates (5×10^3 cells/well) and then incubated with DMEM containing 0.3% BSA and PDGF-BB (10 ng/mL) (PeproTech EC, UK) for 3 days. Cell numbers per well were counted with the use of the Cell Counting Kit-8 (Dojindo, Kumamoto, Japan).

The migration assay was performed with Transwell (Corning, Nagog, MA) 24-well tissue culture plates composed of an 8 μm pore polycarbonate membrane. The inner chamber membrane was coated with 0.1% gelatin. SMCs were then seeded on the inner chamber of the Transwell at a concentration of 5×10^3 cells/100 μL. The inner chamber was placed into the outer chamber containing recombinant human PDGF-BB (10 ng/mL), and then incubated for 6 h at 37 °C. The cells that migrated onto the outer side of the membrane were fixed and stained. The number of migrated cells was counted in the five ran-

domly chosen fields of the duplicated chambers at a magnification of 200× for each sample.

Cuff-induced intimal thickening of the murine femoral artery. The cuff placement surgery was performed according to a method and the sections were stained and measured as described [16]. After the experimental period, the mice were euthanized, and their arterial tissues were fixed in 10% formalin and then embedded in paraffin. The middle segment of the artery was cut into five subserial cross-sections at intervals of 200 μm. The sections were stained using elastica van Gieson or hematoxylin and eosin staining. The areas of the neointima, media, and adventitia were measured utilizing image-analyzing software (NIH Image). To evaluate DNA synthesis, bromodeoxyurine (BrdU, Sigma–Aldrich, St. Louis, MO) was injected at doses of 100 mg/kg SC and 30 mg/kg IP 18 h before euthanasia and then at a dose of 30 mg/kg IP 12 h before euthanasia. Immunohistochemistry using anti-BrdU antibody (Dako, Carpinteria, CA) in serial sections was performed and BrdU index (the ratio of BrdU-positive nuclei versus total nuclei) was calculated.

Statistical analysis. Values are given as means ± SEM. All comparisons were done using the Student's *t* test for comparisons between groups. $P < 0.05$ is considered significant, and $P < 0.01$ was considered highly significant.

Results

Establishment of Ayu8025 line and identification of trapped gene

We isolated gene trap ES clones using the trap vector pU-Hachi and established 36 mouse trap mouse lines through the production of germline chimeras. We screened these mice by whole mount X-gal staining using embryonic days (E) 12.5 embryos. Interestingly, one of these lines, Ayu8025, showed strong expression of *lac*Z in blood vessels such as vitelline vessels (Fig. 1A) and thus this was further investigated. This mutant mouse line was designated as B6; CB-Abhd2^{GtAyu8025IMEG}. To identify the gene trapped and characterize the insertion site of the trap vector, we performed 5′ RACE and plasmid rescues. The trap vector was inserted into the fifth intron of the *Abhd2* gene. We confirmed that the integration of the trap vector resulted in the deletion of 634 bp of genomic DNA located at nucleotide positions between 63,583 and 64,216 (Fig. 1B). In addition, 2 or 14 bp were deleted from the 5′ end or the 3′ end of the trap vector, respectively. A tail DNA was used for genotyping by PCR. For the wild-type allele, the G1 primer and the G2 primer were used to generate a 663 bp wild-type fragment. To detect the trap allele, the G3 primer and the G2 primer were used to generate a 425 bp fragment. Using these primers, the genotype of the offspring from the heterozygous inter-cross was easily identified (Fig. 1C). Heterozygous and homozygous mice appeared normal and were fertile. Even at the nineth backcross generation to C57BL/6, 46 homozygous, 114 heterozygous, and 48 wild-type mice were generated among 208 live-born offspring by mating between heterozygote parents. This ratio was consistent with the expected Mendelian distribution.

Northern blot and RT-PCR analyses

In order to examine the tissue specific expression and presence of fusion transcripts, the Northern blot analyses using various adult tissues, including brains, hearts, lungs, livers, spleens, skeletal muscles, kidneys, testes, uteruses, and aortas of wild-type, heterozygous and homozygous mice were performed using a fragment of the *Abhd2* cDNA as a probe. In wild-type mice, 6.8 kb transcripts were detected in all tissues examined except for skeletal muscle (Fig. 2A), although the level of expression was variable among these tissues. This 6.8 kb transcript consists of 1.6 kb of *Abhd2* ORF and 5.2 kb of the 3′ UTR region as confirmed by analysis of 3′ RACE products. In heterozygous mice, two bands of 6.8 and 5.2 kb were detected (Fig. 2A). In homozygous mutant mice, the 5.2 kb transcripts were detected in the same tissues (Fig. 2A) as in the wild-type mice.

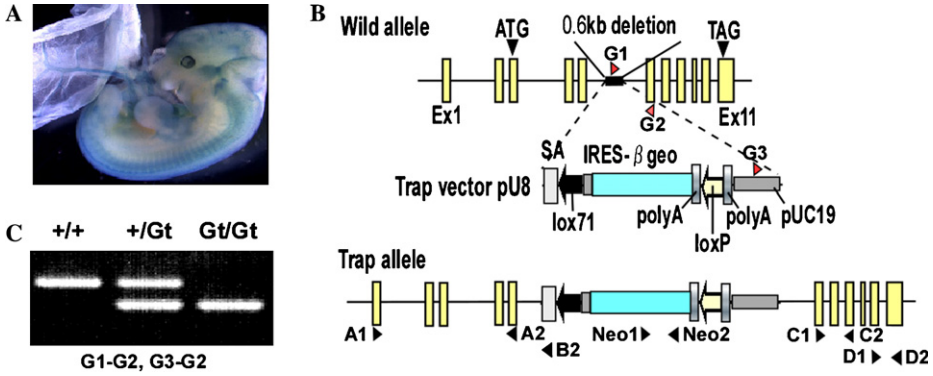

Fig. 1. Insertional mutation of *Abhd2* gene. (A) Expression of *lac*Z at E12.5. X-gal is positive for vitelline vessels in the yolk sac and other tissues including somites. (B) Structure of the wild-type and trap alleles. The trap vector, pU8, was inserted into the fifth intron of the *Abhd2* gene, resulting in a loss of 0.6 kb intronic sequences. The red arrowheads, G1, G2, and G3, are used for the genotyping of mice. Black arrowheads, A1, A2, B2, C1, C2, D1, D2, Neo1, and Neo2, are used for RT-PCR. (C) PCR genotyping. The wild-type or trap allele is detected using G1 and G2 or G1 and G3 primer sets, respectively. +/+, wild-type mouse; +/Gt, heterozygous mouse; Gt/Gt, homozygous mutant mouse.

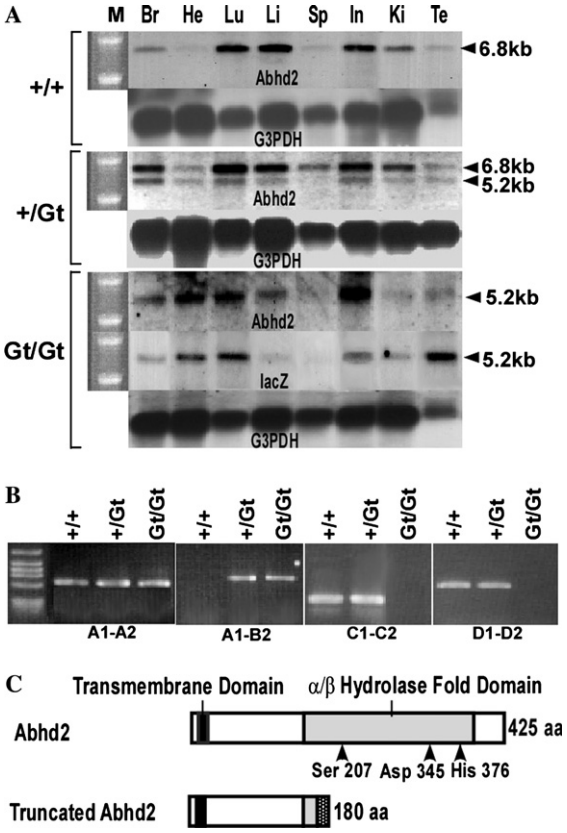

Fig. 2. Disruption of *Abhd2* expression in mutant mice. (A) Northern blot analyses of wild-type (+/+), heterozygous (+/Gt), and homozygous mutant (Gt/Gt) mice. In the +/+ mouse, only a 6.8 kb band was detected in various tissues. In the +/Gt mouse, both 6.8 and 5.2 kb bands were detected. In the Gt/Gt mouse, only a 5.2 kb band which was hybridized with both *Abhd2* and *lac*Z probes was detected. These result suggest that the insertion of trap vector results in the complete loss of wild-type mRNA and in the production of 5.2 kb fusion mRNA. (B) RT-PCR analyses using primers shown in Fig. 1B. Using probes A1 and A2, 558 bp products were detected in +/+, +/Gt, and Gt/Gt mice. Using probes A1 and B2, 724 bp products were only detected in mice carrying the trap allele. When probes C1 and C2 or D1 and D2 were used, 302 or 392 bp products were detected, respectively, in +/+ and +/Gt mice, but not in Gt/Gt mouse. These results suggest that no other alternative splicing occurs in either the wild-type or the trap allele. (C) Schematic diagram of wild-type and truncated *Abhd2* protein. Truncated *Abhd2* protein lacks most of α/β hydrolase fold domain. Arrowheads indicate triad catalytic domains (Ser207, Asp345, and His376). M, size marker; Br, brain; He, heart; Lu, lung; Li, liver; Sp, spleen; In, intestine; Ki, kidney; Te, testis.

The 5.2 kb transcripts were also hybridized with the *lac*Z probe (Fig. 2A), suggesting that this transcript is a fusion message comprised of 0.5 kb truncated *Abhd2* and 4.7 kb *β-geo* mRNA. This was confirmed by sequencing the 5′ RACE product.

To examine whether any other alternative splicing product was present or not, RT-PCR analyses were done using probes as described in Materials and methods. Using probes A1 and A2, 558 bp products were detected in wild-type, heterozygous, and homozygous mice (Fig. 2B). As expected, 724 bp products were only detected in mice carrying the trap alleles when probes A1 and B2 were used (Fig. 2B). When probes C1 and C2 or D1 and D2 were used, 302 or 392 bp products were detected, respectively, in wild-type and heterozygous mice (Fig. 2B). These results suggest that no other alternative splicing occurs in either the wild-type or trap allele. Thus, the insertion of a trap vector into the fifth intron results in the complete loss of the wild-type message and in the transcription of a fusion message. As the fusion message contains up to the fifth exon, it was expected to produce a truncated Abhd2 protein that contains only 180 amino acids of N-terminus, but not the catalytic domain of α/β hydrolase fold protein (Fig. 2C).

Analysis of X-gal staining

To analyze cell-type specific expression of the *Abhd2* gene, we performed X-gal staining using tissue sections of adult mice. It is noteworthy that β-galactosidase activity was detected in vascular SMCs, non-vascular SMCs, and the heart, but not in the skeletal muscle cells. Vascular SMCs include those in the aorta (Fig. 3A), small arteries in the skin (arrow in Fig. 3B), arterioles in the ear (arrow in Fig. 3C), and in superior and inferior vena (Fig. 3D). The *lac*Z expression was not detected in veins (arrowhead in Figs. 3B and C), probably because of absence of SMCs. *lac*Z was also expressed in the myocardium of the atrium and ventricles of the heart (Fig. 3E) and in the non-vascular smooth muscle cells such as the bronchial SMC layers (Fig. 3F), uterine SMCs (Fig. 3G), intestinal SMC layers (Fig. 3K), and bladder SMCs (data not shown); however, *lac*Z was not detected in the skeletal muscle cells (Fig. 3H). We confirmed that X-gal positive cells were indeed vascular or non-vascular SMCs, but not endothelial cells, utilizing immuno-histochemical staining with anti-α-smooth muscle actin antibodies (Figs. 3I, J, K, and L). In situ hybridization experiments using the same 5′ probe as used for the Northern blot analysis (see Fig. 1) revealed that X-gal positive cells were coincident with those cells that expressed the mouse *Abhd2* mRNA (data not shown), suggesting that *lac*Z staining reflects the expression pattern of the *Abhd2* gene.

X-gal positive cells were also detected in other types of cells, such as hepatocytes around hepatic interlobular areas of liver tissue (Fig. 3M), alveolar type II cells of lung tissue (Fig. 3N), splenic cords (reticular cells) around white pulp in the spleen (Fig. 3O), the cortex area of adrenal gland (Fig. 3P) and other tissues such as islet cells of Langerhans of the pancreas or columnar epithelium cells in ductus deferens (data not shown). In the brain, X-gal was positive in epithelium cells of choroids, granular cells of gyrus dentatus, and external and internal granular cells of the cerebral cortex (data not shown).

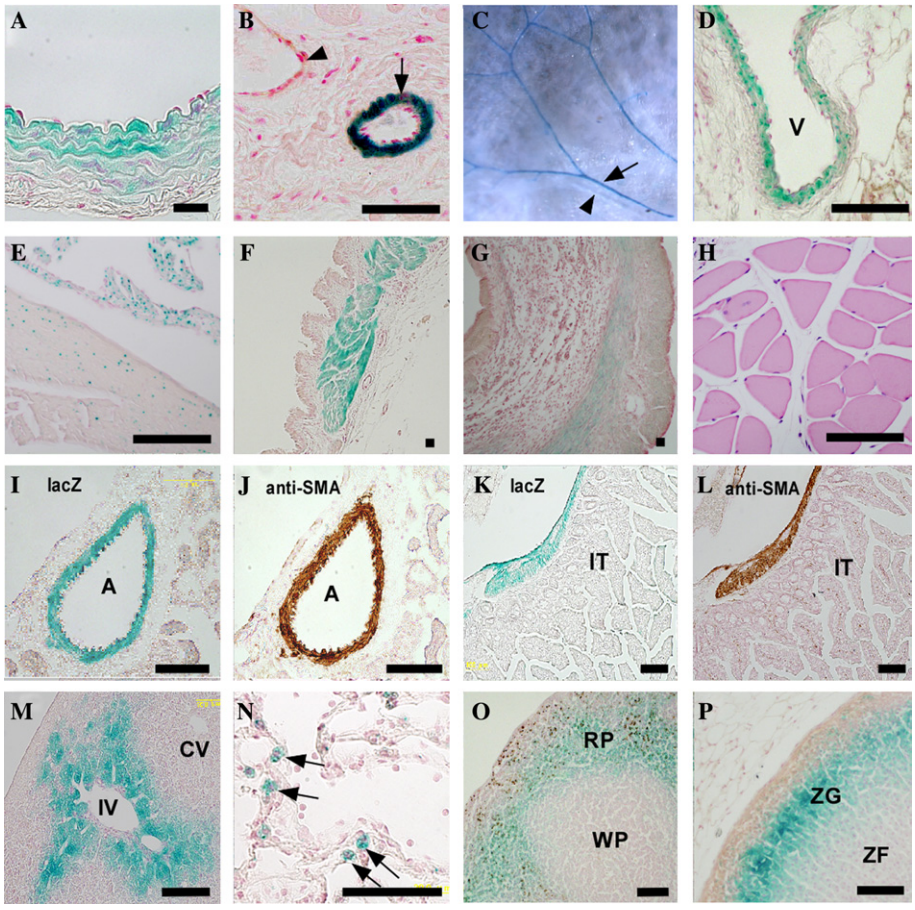

Fig. 3. X-gal staining in heterozygous mice. *Lac*Z expression was detected in vascular SMCs of the aorta (A), small arteries in the skin (arrow in B), arterioles in the ear (C), superior and inferior vena (D), but not in veins (arrowheads in B and C). *Lac*Z was also expressed in the myocardium of the atrium and in the ventricle of the heart (E) and non-vascular smooth muscle cells, such as the bronchial SMC layer (F), uterine SMCs (G), and intestinal SMC layer (K); however, *lac*Z was not detected in skeletal muscle cells (H). X-gal positive cells are clearly stained with anti-α-smooth muscle actin antibody in both vascular (I, J) or non-vascular tissues (K, L). X-gal positive cells were also detected in other types of cells, such as the hepatocytes around hepatic interlobular area of liver tissue (M), alveolar type II cells of lung tissue (arrows in N), splenic cords (reticular cells) around white pulp in the spleen (O), and the cortex area of the adrenal gland (P). A, artery; V, vein; IT, intestinal tract; IV, interlobular vein; CV, central vein; RP, red pulp; WP, white pulp; ZG, zona glomerulosa; ZF, zona fasciculata. Scale bar = 100 μm

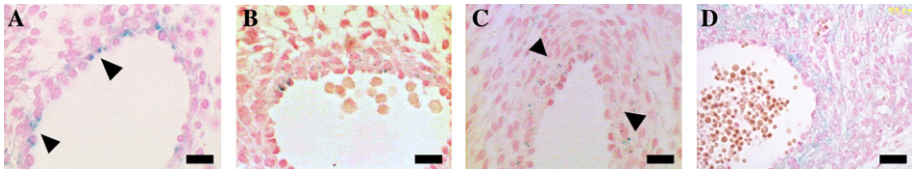

Fig. 4. Developmental expression of *lac*Z in the aorta. At E10.5, *lac*Z was expressed in endothelial cells of the dorsal aorta, but not in SMCs (A) At E11.5, *lac*Z expression was detected in both endothelial cells and in SMCs (B) At E13.5, *lac*Z was expressed in most of the SMCs (C) At E16.5, *lac*Z was expressed in all SMCs, but in only a few endothelial cells (D). Thus, the expression of *Abhd2* starts in endothelial cells, and then shifts to SMCs during embryonic development. Arrowheads indicate the *lac*Z positive cells. Scale bar = 25 μm.

Developmental expression of LacZ

As the most characteristic feature of the *Abhd2* is its expression in vascular smooth muscle cells, we examined the developmental expression of *Abhd2* utilizing X-gal staining on heterozygous embryos. At embryonic day 9.5 (E9.5), weak β-galactosidase expression was detected in the heart. At E10.5 *lac*Z was expressed in the endothelial cells of the dorsal aorta (Fig. 4A), but not in SMCs. This *lac*Z expression in the endothelial cells disappeared by E12.5. In contrast, *lac*Z expression was first detected in SMCs at E11.5 (Fig. 4B). At E13.5, *lac*Z was being expressed in most of SMCs (Fig. 4C). By E16.5, *lac*Z was expressed in all SMCs (Fig. 4D). Thus, *Abhd2* starts

to be expressed in the endothelial cells, and then its expression shifts into SMCs during E10.5–E13.5.

Function of Abhd2 in vitro and in vivo

Although X-gal staining revealed specific expression of *Abhd2* in vascular SMCs, homozygous mutant mice did not show any over phenotype. Thus, we investigated the role of *Abhd2* on the migration and proliferation of vascular SMCs. To investigate the ability of PDGF-BB-directed SMCs to migrate across Transwell filters, an explant culture method using mouse SMCs derived from either wild-type or homozygous mutant mice was used. We found that the number of cells that passed through the filters in the presence of gradient of chemo-attractant in homozygotes was 140 ± 22.3 SMCs/field which was significantly higher than the 78.8 ± 17.7 SMCs/field in wild-type mice ($P < 0.05$; (Fig. 5A)).

In the proliferation assay, there was no difference in the PDGF-BB-induced proliferative response of cultured SMCs derived from either wild-type or homozygote (Fig. 5B). These data suggest that *Abhd2* is

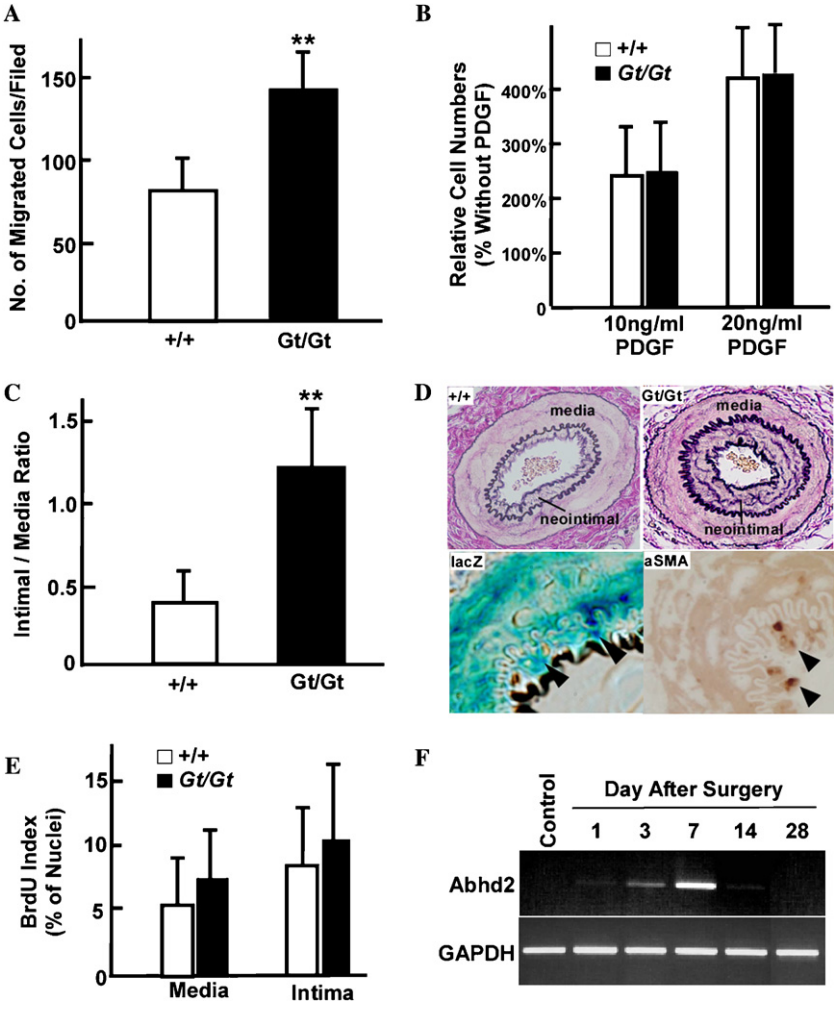

Fig. 5. Function of *Abhd2* in vitro and in vivo. Cultured SMCs derived from the aortas of wild-type and *Abhd2* deficient mice were used for experiments. (A) Transwell assay for SMC migration in the presence of PDGF-BB. The number of cells that passed through the filters in the presence of PDGF-BB (10 ng/mL) in homozygous (Gt/Gt) mice was 140 ± 22.3 SMCs/field which was significantly higher than 78.8 ± 17.7 SMCs/field in the wild-type (+/+) mice ($P < 0.05$). (B) Proliferative ability of SMCs from wild-type or homozygous mice. Data are expressed as a percentage of the cell number in SMCs incubated with culture medium without PDGF-BB. There was no difference in the PDGF-BB-induced proliferative response of cultured SMCs derived from wild-type or homozygous mice. (C) The intimal/media ratio at 28 days after cuff placement. Intimal/media ratio was significantly larger in homozygous mice than in wild-type mice. (D) Sections of the femoral arteries 28 days after cuff placement of wild-type and homozygous mice stained with elastica van Gieson, X-gal, and anti-αSMA antibody. Neointimal thickening was significantly larger in homozygous mice than in wild-type mice, while the adventitial region was similar between them. Cells in the neointimal area expressing *lacZ* (blue) and α smooth muscle actin (blue) are indicated by arrowheads. (E) BrdU uptakes in both the intimal and the medial layers. BrdU uptakes in both intimal and medial layers were not different between the wild-type and homozygote mice. (F) Time course of *Abhd2* mRNA expression after cuff placement. Expression of *Abhd2* increased and reached a maximum level at 7 days and then decreased to an undetectable level by 14 days after cuff placement of the femoral artery. Glyceraldehyde-3-phosphate dehydrogenase (GAPDH) was used as an internal control. Quantitative analysis of the area of explant culture and intimal/media was performed with the NIH Image software. Results represent means ± SEM of eight experiments. $^{**}P < 0.01$e.

involved in the regulation of SMC migration in response to exogenous factors; therefore, we investigated the in vivo role of *Abhd2* on vascular smooth muscles using the cuff placement model. To examine the effect of cuff placement on the neointimal formation, we analyzed histological sections. In the sham-operated side, no neointimal thickening was found at 7 days or 28 days after surgery in either wild-type or homozygous mice. In the cuff placement side, no neointimal hyperplasia was found at 7 days after surgery in either wild-type or homozygote mice; however, at 28 days after surgery, neointimal hyperplasia was observed in both wild-type and homozygote mice. Neointimal thickening was significantly larger in homozygous mice than in wild-type mice, while the adventitial region was similar between them (Figs. 5C and D). Cells in the neointimal area expressed *lac*Z and α smooth muscle actin (Fig. 5D).

To analyze the proliferative activity of SMCs, DNA synthesis was examined by BrdU uptake 7 days after cuff injury. BrdU uptakes in both intimal and medial layers were not different between the wild-type or homozygote mice (Fig. 5E). Taken together, neointimal hyperplasia in homozygous mice might be caused by the migration of SMCs, but not by the proliferation of SMCs. If the absence of the *Abhd2* expression is involved in enhanced migration of SMCs, the expression of *Abhd2* should be increased after cuff placement in wild-type mice. Thus, we analyzed the time course of *Abhd2* mRNA expression after cuff injury. RT-PCR analysis showed that expression of *Abhd2* increased and reached a maximum level at 7 days after cuff injury of the femoral artery (Fig. 5F). These data indicated that the loss of *Abhd2* resulted in the enhancement of vascular SMCs migration, leading to the neointimal hyperplasia.

Discussion

We have established the Ayu8025 trap mutant line in which the trap vector was inserted into the fifth intron of the *Abhd2* gene, which is one of the α/β hydrolase protein family. This insertion results in the production of fusion transcript which can produce truncated proteins containing 180 amino acids, but lacking triad catalytic triad domains (Ser207, Asp345, and His376) of the *Abhd2* protein. Thus, truncated *Abhd2* protein may lose its function; however, *Abhd2* deficient mice have no obvious phenotype under normal conditions. The ESTHER, the database of the α/β hydrolase fold superfamily of proteins, reported that mouse *Abhd2* protein belongs to the upf_0017subfamily of the α/β hydrolase fold family including mouse *Abhd1* and *Abhd3* [17]. The NCBI database just reported the data on mouse *Abhd4* and *Abhd6*. Further study to examine the cell-type specific expression of these family genes will be required to assess the possibility that these genes can compensate for a deficiency of *Abhd2*.

From our findings on *Abhd2* expression in vascular SMCs, we performed two experiments to study the function of the *Abhd2* gene. First, the in vitro study demonstrated that the migratory ability of cultured SMCs from *Abhd2* deficient mice was higher than that of wild-type mice. The proliferation ability showed no significant difference between them. This indicates that *Abhd2* plays a critical role for regulating SMC migration. Second, we investigated the role of *Abhd2* in vivo, using the cuff placement model in the mouse femoral artery. *Abhd2* deficient mice showed a marked increase in neointimal area in comparison with that of wild-type mice. On the other hand, there was no difference in the PDGF-BB-induced proliferative response of cultured SMCs derived from either wild-type or homozygote in terms of BrdU labeling in either the intimal or the media region. These results suggest that increased SMC migratory activity is the main cause for the increase of intimal hyperplasia in *Abhd2* deficient mice. However, other growth factors or molecules such as hyaluronic acid, heparin or aminoglycan chains of heparan sulfate proteoglycans, are also reported to affect SMC's migration and proliferation after vascular injury. For example, SMCs secrete a hyaluronic acid into extracellular matrix and hyaluronic acid was involved vascular injury model [18]. Papakonstantinou et al. [19,20] reported that hyaluronic acid plays a role of positive regulator on the PDGF-BB induced SMC proliferation. To investigate the roles of these molecules and the extracellular matrix, further studies using our mouse line will be required.

The mechanisms of intima formation after the cuff placement model are not known yet. Previous studies have shown that medial SMCs are modified and migrate into the intima, where they proliferate and secrete extracellular matrix components [21], and that adventitial fibroblasts migrate into the neointima and differentiate into SMC-like cells [22]. Recently, Tanaka et al. [23] reported that in the cuff placement model bone marrow-derived cells are seldom detected in the neointima, whereas many inflammatory cells in the adventitia are derived from bone marrow cells. Yang et al. also found that the neointimal formation was caused by an interaction and differentiation between macrophages and SMCs in the adventitia area [24]. From these studies, it is not certain that neointimal cells, which express *Abhd2*, migrate from adult bone marrow containing multipotent cells.

Several α/β hydrolase protein family relations to atherosclerosis have been reported. N-myc downstream regulated gene 4 (Ndrg4), also known as smooth muscle-associated protein 8 (smap8) belongs to the α/β hydrolase protein family as predicted from nucleotide sequences. Nishimoto et al. demonstrated that *Ndrg4* expression in vascular SMCs is highly induced by homo-

cysteine. Homocysteine, a sulfur-containing amino acid, is an intermediate metabolite of methionine and is widely recognized as an independent risk factor for atherogenesis [1,25], because patients with severe homocysteinemia suffer from arterial and venous thromboembolic events at an early age. Although overexpression of *Ndrg4* decreased the proliferation and migration of rat aortic smooth muscle cells (A10 cells), PDGF-induced proliferation was significantly enhanced in *Ndrg4* expressed cells. These results suggest that *Ndrg4* is involved in the regulation of mitogenic signaling in vascular SMCs, possibly in response to a homocysteine-induced injury. Soluble epoxide hydrolase (sEH, previously called cytosolic epoxide hydrolase) plays a role in the xenobiotic metabolism and its substrate is epoxyeicosatrienoic acids (EETs), which are synthesized by endothelial cells, and taken up by vascular SMCs. EETs control vascular tone and contribute to pathogenesis of atherosclerosis. sEH is critical in the control of EET levels and inhibitors of sEH have been reported to attenuate vascular SMC proliferation [2,26–28]; furthermore, the human polymorphism of sEH has been reported to be associated with atherosclerosis [4]. Chen et al. cloned retinoid-inducible serine carboxypeptidase (RISC) from vascular SMCs as a target molecule by retinoids. Retinoids are involved in the vascular response to injury and blocks SMC proliferation and attenuates neointimal hyperplasia formation after injury [29]. Taken together, these studies suggest that these α/β hydrolase proteins influence the behavior of vascular SMC and therefore cause vascular disease.

Interestingly, *Abhd2* is expressed in alveolar type II cells of the lung and hepatocytes around the interlobular area of the liver. *Abhd* family genes were identified in a gene screen of human emphysematous tissue [7]. This suggests that *Abhd2* is related to lung homeostasis. Actually, microsomal epoxide hydrolase, one of α/β hydrolase protein family, was expressed in the alveolar epithelial cells including alveolar type II cells [30] and is associated with the genetic susceptibility for the development of emphysematous changes of the lung [31]. In addition, abnormalities in the surfactant homeostasis of alveolar type II cells are shown to cause the emphysematous change [32]. Our result suggests that *Abhd2* in alveolar type II cells protects alveolar tissues from progressive emphysema, however adult *Abhd2* deficient mice showed no significant structural change in lung tissue. The hepatocytes in the liver are quite heterogeneous in terms of the blood supply. Hepatocytes located in the interlobular zone differ from those in the centrilobular zone. In general, the capacity for oxidative energy metabolism, involved in cell protection, is higher in the interlobular zone and xenobiotic metabolism is higher in the centrilobular zone [33,34]. *Abhd2* was expressed more strongly around portal veins at the interlobular zone, suggesting that *Abhd2* at the interlobular zone protects hepatocytes against exogenous stress factors. Further investigation, such as smoke inhalation experiments or drug administration, may clarify the function of *Abhd2* in the lung or liver.

In conclusion, we find that *Abhd2* contributes to the migration of vascular SMC in the pathologic condition, indicating that *Abhd2* plays an important role in stress response due to external stimulation. Identification of substrates for *Abhd2* will provide an important clue for elucidating the molecular mechanisms of *Abhd2* functioning.

Acknowledgments

This work was supported in part by a Grant-in-Aid on Priority Areas from the Ministry of Education, Science, Culture, and Sports of Japan and a grant from the Osaka Foundation of Promotion of Clinical Immunology.

References

[1] S. Nishimoto, J. Tawara, H. Toyoda, K. Kitamura, T. Komurasaki, A novel homocysteine-responsive gene, smap8, modulates mitogenesis in rat vascular smooth muscle cells, Eur. J. Biochem. 270 (2003) 2521–2531.
[2] B.B. Davis, D.A. Thompson, L.L. Howard, C. Morisseau, B.D. Hammock, R.H. Weiss, Inhibitors of soluble epoxide hydrolase attenuate vascular smooth muscle cell proliferation, Proc. Natl. Acad. Sci. USA 99 (2002) 2222–2227.
[3] J. Chen, J.W. Streb, K.M. Maltby, C.M. Kitchen, J.M. Miano, Cloning of a novel retinoid-inducible serine carboxypeptidase from vascular smooth muscle cells, J. Biol. Chem. 276 (2001) 34175–34181.
[4] M. Fornage, E. Boerwinkle, P.A. Doris, D. Jacobs, K. Liu, N.D. Wong, Polymorphism of the soluble epoxide hydrolase is associated with coronary artery calcification in African-American subjects: The Coronary Artery Risk Development in Young Adults (CARDIA) study, Circulation 109 (2004) 335–339.
[5] D.L. Ollis, E. Cheah, M. Cygler, B. Dijkstra, F. Frolow, S.M. Franken, M. Harel, S.J. Remington, I. Silman, J. Schrag, et al., The α/β hydrolase fold, Protein Eng. 5 (1992) 197–211.
[6] M. Holmquist, α/β-hydrolase fold enzymes: Structures, functions, and mechanisms, Curr. Protein Pept. Sci. 1 (2000) 209–235.
[7] A.J. Edgar, J.M. Polak, Cloning and tissue distribution of three murine α/β hydrolase fold protein cDNAs, Biochem. Biophys. Res. Commun. 292 (2002) 617–625.
[8] M.J. Evans, M.B. Carlton, A.P. Russ, Gene trapping and functional genomics, Trends Genet. 13 (1997) 370–374.
[9] A. Gossler, A.L. Joyner, J. Rossant, W.C. Skarnes, Mouse embryonic stem cells and reporter constructs to detect developmentally regulated genes, Science 244 (1989) 463–465.
[10] K. Araki, T. Imaizumi, T. Sekimoto, K. Yoshinobu, J. Yoshimuta, M. Akizuki, K. Miura, M. Araki, K. Yamamura, Exchangeable gene trap using the Cre/mutated lox system, Cell. Mol. Biol. (Noisy-le-grand) 45 (1999) 737–750.
[11] Y. Oike, N. Takakura, A. Hata, T. Kaname, M. Akizuki, Y. Yamaguchi, H. Yasue, K. Araki, K. Yamamura, T. Suda, Mice homozygous for a truncated form of CREB-binding protein exhibit defects in hematopoiesis and vasculo-angiogenesis, Blood 93 (1999) 2771–2779.

[12] T. Imaizumi, K. Araki, K. Miura, M. Araki, M. Suzuki, H. Terasaki, K. Yamamura, Mutant mice lacking Crk-II caused by the gene trap insertional mutagenesis: Crk-II is not essential for embryonic development, Biochem. Biophys. Res. Commun. 266 (1999) 569–574.
[13] Y. Kawazoe, T. Sekimoto, M. Araki, K. Takagi, K. Araki, K. Yamamura, Region-specific gastrointestinal Hox code during murine embryonal gut development, Dev. Growth Differ. 44 (2002) 77–84.
[14] Y. Yamauchi, K. Abe, A. Mantani, Y. Hitoshi, M. Suzuki, F. Osuzu, S. Kuratani, K. Yamamura, A novel transgenic technique that allows specific marking of the neural crest cell lineage in mice, Dev. Biol. 212 (1999) 191–203.
[15] M. Kuzuya, A. Iguchi, Role of matrix metalloproteinases in vascular remodeling, J. Atheroscler. Thromb. 10 (2003) 275–282.
[16] Y. Imai, T. Shindo, K. Maemura, M. Sata, Y. Saito, Y. Kurihara, M. Akishita, J. Osuga, S. Ishibashi, K. Tobe, H. Morita, Y. Ohhashi, T. Suzuki, H. Maekawa, K. Kangawa, N. Minamino, Y. Yazaki, R. Nagai, H. Kurihara, Resistance to neointimal hyperplasia and fatty streak formation in mice with adrenomedullin overexpression, Arterioscler. Thromb. Vasc. Biol. 22 (2002) 1310–1315.
[17] T. Hotelier, L. Renault, X. Cousin, V. Negre, P. Marchot, A. Chatonnet, ESTHER, the database of the α/β-hydrolase fold superfamily of proteins, Nucleic Acids Res. 32 (2004) D145–D147 (Database issue).
[18] R.C. Savani, C. Wang, B. Yang, S. Zhang, M.G. Kinsella, T.N. Wight, R. Stern, D.M. Nance, E.A. Turley, Migration of bovine aortic smooth muscle cells after wounding injury. The role of hyaluronan and RHAMM, J. Clin. Invest. 95 (1995) 1158–1168.
[19] E. Papakonstantinou, G. Karakiulakis, M. Roth, L.H. Block, Platelet-derived growth factor stimulates the secretion of hyaluronic acid by proliferating human vascular smooth muscle cells, Proc. Natl. Acad. Sci. USA 92 (1995) 9881–9885.
[20] E. Papakonstantinou, M. Roth, L.H. Block, V. Mirtsou-Fidani, P. Argiriadis, G. Karakiulakis, The differential distribution of hyaluronic acid in the layers of human atheromatic aortas is associated with vascular smooth muscle cell proliferation and migration, Atherosclerosis 138 (1998) 79–89.
[21] A.C. Newby, A.B. Zaltsman, Molecular mechanisms in intimal hyperplasia, J. Pathol. 190 (2000) 300–309.
[22] A. Zalewski, Y. Shi, Vascular myofibroblasts. Lessons from coronary repair and remodeling, Arterioscler. Thromb. Vasc. Biol. 17 (1997) 417–422.
[23] K. Tanaka, M. Sata, Y. Hirata, R. Nagai, Diverse contribution of bone marrow cells to neointimal hyperplasia after mechanical vascular injuries, Circ. Res. 93 (2003) 783–790.
[24] Y. Xu, H. Arai, X. Zhuge, H. Sano, T. Murayama, M. Yoshimoto, T. Heike, T. Nakahata, S. Nishikawa, T. Kita, M. Yokode, Role of bone marrow-derived progenitor cells in cuff-induced vascular injury in mice, Arterioscler. Thromb. Vasc. Biol. 24 (2004) 477–482.
[25] M.R. Malinow, P.B. Duell, D.L. Hess, P.H. Anderson, W.D. Kruger, B.E. Phillipson, R.A. Gluckman, P.C. Block, B.M. Upson, Reduction of plasma homocyst(e)ine levels by breakfast cereal fortified with folic acid in patients with coronary heart disease, N. Engl. J. Med. 338 (1998) 1009–1015.
[26] N. Chacos, J. Capdevila, J.R. Falck, S. Manna, C. Martin-Wixtrom, S.S. Gill, B.D. Hammock, R.W. Estabrook, The reaction of arachidonic acid epoxides (epoxyeicosatrienoic acids) with a cytosolic epoxide hydrolase, Arch. Biochem. Biophys. 223 (1983) 639–648.
[27] X. Fang, T.L. Kaduce, N.L. Weintraub, M. VanRollins, A.A. Spector, Functional implications of a newly characterized pathway of 11,12-epoxyeicosatrienoic acid metabolism in arterial smooth muscle, Circ. Res. 79 (1996) 784–793.
[28] M. Rosolowsky, W.B. Campbell, Synthesis of hydroxyeicosatetraenoic (HETEs) and epoxyeicosatrienoic acids (EETs) by cultured bovine coronary artery endothelial cells, Biochim. Biophys. Acta 1299 (1996) 267–277.
[29] D.I. Axel, A. Frigge, J. Dittmann, H. Runge, I. Spyridopoulos, R. Riessen, R. Viebahn, K.R. Karsch, All-*trans*-retinoic acid regulates proliferation, migration, differentiation, and extracellular matrix turnover of human arterial smooth muscle cells, Cardiovasc. Res. 49 (2001) 851–862.
[30] K. Takeyabu, E. Yamaguchi, I. Suzuki, M. Nishimura, N. Hizawa, Y. Kamakami, Gene polymorphism for microsomal epoxide hydrolase and susceptibility to emphysema in a Japanese population, Eur. Respir. J. 15 (2000) 891–894.
[31] C.A. Smith, D.J. Harrison, Association between polymorphism in gene for microsomal epoxide hydrolase and susceptibility to emphysema, Lancet 350 (1997) 630–633.
[32] M. Sulkowska, S. Sulkowski, J. Dzieciol, Type II alveolar epithelial cells promote fibrosis during development of experimental lung emphysema, Folia Histochem. Cytobiol. 34 (Suppl. 1) (1996) 27–28.
[33] R.G. Thurman, F.C. Kauffman, Sublobular compartmentation of pharmacologic events (SCOPE): Metabolic fluxes in periportal and pericentral regions of the liver lobule, Hepatology 5 (1985) 144–151.
[34] T. Kietzmann, K. Jungermann, Modulation by oxygen of zonal gene expression in liver studied in primary rat hepatocyte cultures, Cell Biol. Toxicol. 13 (1997) 243–255.